

Polarization transfer in the (p, p') reaction on light nuclei

W. D. Cornelius,* J. M. Moss,* and T. Yamaya

Cyclotron Institute and Physics Department, Texas A&M University, College Station, Texas 77843

(Received 29 September 1980)

A high-efficiency, high-resolution polarimeter has been employed to measure the transverse spin-flip probability in (p, p') reactions induced by polarized protons in the energy range from 30 to 42 MeV. The spin-flip probability for central forces is shown to be uniquely related to spin transfer ($s = 1$) in the eikonal approximation. More exact calculations indicate the general rule $S \geq 0.5$ when $s = 1$ and $S \leq 0.1$ when $s = 0$. Antisymmetrized distorted-wave calculations give a generally poor account of spin transfer in isoscalar transitions and transitions in odd mass nuclei. Spin flip in isovector transitions is well described by the calculations.

[NUCLEAR REACTIONS ${}^6\text{Li}$, ${}^9\text{Be}$, ${}^{11}\text{B}$, ${}^{12}\text{C}$, ${}^{14}\text{N}$, ${}^{16}\text{O}$, and ${}^{40}\text{Ca}(p, p')$, $E_p = 31, 32, 35.5, 40, 42$ MeV, measured spin-flip probabilities.]

I. INTRODUCTION

A. General

Since the advent of high intensity polarized ion sources, it has been routinely possible to measure analyzing powers in inelastic proton scattering reactions. Such studies have led to interesting and important refinements of collective models of inelastic scattering.¹ However, analyses of inelastic analyzing powers using various microscopic models have contributed essentially nothing to our knowledge either of nuclear wave functions or to the phenomenology of the effective nucleon-nucleon ($N-N$) interaction. The reasons for these observations are now clear. The vector analyzing power in (p, p') reactions is overwhelmingly dominated by the deflection of the proton's trajectory by the nucleon-nucleus spin-orbit (SO) potential. The collective model, an extension of the spherical optical model, describes this process in a consistent manner for those nuclear states which can be viewed as collective. In the microscopic view of inelastic scattering where the effects of tensor, spin-spin, and two body SO forces are sought, the "background" analyzing power from the optical potential's SO field obscures any contribution from valence nucleons, thus rendering the interpretation of the data very ambiguous.

Because the role of spin in nuclear structure and the closely related problem of the spin dependence of the residual $N-N$ interaction are of general interest in nuclear physics, it is important to know what polarization observable might shed light on these problems. In three previous publications²⁻⁴ we have suggested that the spin-flip (SF) probability in inelastic scattering is the appropriate

quantity because it is very weakly influenced by the SO potential. We shall show in Sec. IB that the SF probability is large only when spin transfer ($s = 1$) dominates the (p, p') process. Spin transfer in turn is mediated largely by the central spin-dependent and tensor components of the effective $N-N$ interaction. The action of these spin-independent forces in inelastic hadron scattering is closely related to magnetic transitions observed in electron scattering. Spin flip in inelastic scattering reactions should thus provide a new tool for the elucidation of these very interesting and relatively poorly known transitions.

B. Spin dependent forces, spin transfer, and the spin flip probability

In a coordinate system with the z axis along $\vec{k}_a \times \vec{k}_b$ (incoming and outgoing momenta respectively), the SF probability S can be expressed in terms of the transition amplitude $\beta_{l'sj}^{m_a, m_b}$ in an intuitively transparent way. Neglecting antisymmetrization

$$S = \frac{\sum |\beta_{l'sj}^{m_a, m_b}|}{D} \tag{1.1}$$

where using the notation of Statchler,⁵ $m_a(m_b)$ is the initial (final) projection of the proton spin and m is the projection of l . The summation is over $l, s, j, m, m_a \neq m_b$; the denominator D is identical to the numerator with the exception that the summation over m_a and m_b is unrestricted. Neglect of the weak coherence between l and s provided by the SO force allows the total SF probability to be approximated by

$$S = \frac{\sum_{i,s,j} (d\sigma/d\Omega)_{i,s,j} S_{i,s,j}}{\sum_{i,s,j} (d\sigma/d\Omega)_{i,s,j}}, \quad (1.2)$$

where

$$S_{i,s,j} = \frac{\sum |\beta_{i,s,j}^{m_a, m_b}|^2}{D}, \quad (1.3)$$

where the summation is over $m, m_a \neq m_b$ (unrestricted in D). The denominator of Eq. (1.3) is proportional to $(d\sigma/d\Omega)_{i,s,j}$.

If we further restrict ourselves to central forces we can write (Eq. 15 of Ref. 5)

$$\begin{aligned} \beta_{i,s,j}^{m_a, m_b} &= (-)^{s_b - m_b} (2j+1)^{1/2} (2l+1)^{1/2} \\ &\times (lsm, m_a - m_b | jm + m_a - m_b) \\ &\times (s_a s_b m_a - m_b | sm_a - m_b) \beta_{i,s,j}^m, \end{aligned}$$

and neglecting the effects of diffraction in the op-

$$S_{i,s,j} = \frac{\sum_{m, m_a \neq m_b} |(-1)^{m_b} (lsm, m_a - m_b | jm - m_b + m_a) (s_a s_b m_a - m_b | sm_a - m_b) d_{0m}(\pi/2)|^2}{D},$$

where the denominator D contains the same terms but with an unrestricted sum over m_a and m_b .

This reduces to

$$\left. \begin{aligned} S_{i,s,j} &= \frac{3j+1}{2(2j+1)}, \quad j = l+1 \\ S_{i,s,j} &= \frac{3j+2}{2(2j+1)}, \quad j = |l-1| \\ S_{i,s,j} &= \frac{1}{2}, \quad j = l \\ S_{i,s,j} &= 0, \quad s = 0. \end{aligned} \right\} s = 1 \quad (1.4)$$

Thus we find that $S_{i,s,j}$ is dependent only on the angular momentum transfer of the reaction. More importantly we find the $S_{i,s,j}$ is large ($S_{i,s,j} \geq \frac{1}{2}$) when $s = 1$ and zero when $s = 0$). Because spin transfer only occurs when there is a coupling between the spin operators of the interacting nucleons, $S_{i,s,j}$ is large (small) only if spin-dependent forces are present (absent) in a given inelastic transition.

Although a number of simplifications have been made in arriving at Eq. (1.4), more realistic distorted-wave calculations strongly confirm the conclusion that spin flip is a reliable indicator of the action of spin-dependent forces in the forward angle region ($\theta_{c.m.} < 100^\circ$). At backward angles the SO distortion can produce a large and experiment-

tical potential (i.e., the eikonal approximation) we have

$$\beta_{i,s,j}^m = \beta_{i,s,j}^m \delta_{m0}$$

provided the quantization axis is chosen to coincide with $\vec{q} = \vec{k}_a - \vec{k}_b$. In order to use Eq. (1.3) to calculate $S_{i,s,j}$ we need to rotate this transition amplitude to the frame with z along $\vec{k}_a \times \vec{k}_b$. This is accomplished by (Ref. 5, Eq. A5)

$$\begin{aligned} \beta_{i,s,j}^m(\vec{k}_a \times \vec{k}_b) &= \sum_m \beta_{i,s,j}^{m'}(\vec{q}) D_{m' m}^i(0, \pi/2, 0) \\ &= \beta_{i,s,j}^0(\vec{q}) d_{0m}^i(\pi/2). \end{aligned}$$

Note that the dependence of the original reaction amplitude on the summation indices m, m_a , and m_b is entirely contained within the Clebsch-Gordan coefficients and rotation matrix elements. Therefore we can factor $\beta_{i,s,j}^0$ out of Eq. (1.3), with the result

ally well-known peak in the SF probability even when $s = 0$. Figure 1 shows distorted-wave Born approximation (DWBA) calculations for a set of hypothetical states in ^{12}C at $E_p = 30$ MeV. These calculations utilize different single-particle wave functions appropriate for each final state spin and parity [$(p_{3/2}^{-1} p_{1/2})$ or $(p_{3/2}^{-1} f_{7/2})$ for positive parity and $(p_{3/2}^{-1} d_{5/2})$ for negative parity]; however, the results of these calculations are not sensitive to the particular wave function chosen or to the force used.

C. Spin flip and magnetic multipole transitions

The analogy between inelastic scattering with spin transfer and magnetic multipole or beta decay matrix elements has been appreciated for many years.⁶ However, for the sake of clarity we will reiterate the magnetic dipole case.

The isovector and isoscalar $M1$ matrix elements may be written as

$$\text{isovector } M1_1 = (\mu_p - \mu_n + \frac{1}{2}) \sum_i \langle J_B T_B \| T_{3i} \vec{\sigma}_i \| J_A T_A \rangle, \quad (1.5)$$

$$\text{isoscalar } M1_0 = (\mu_p + \mu_n - \frac{1}{2}) \sum_i \langle J_B T_B \| \vec{\sigma}_i \| J_A T_A \rangle,$$

where μ_p and μ_n are, respectively, the magnetic moments of the proton and neutron. (The justifi-

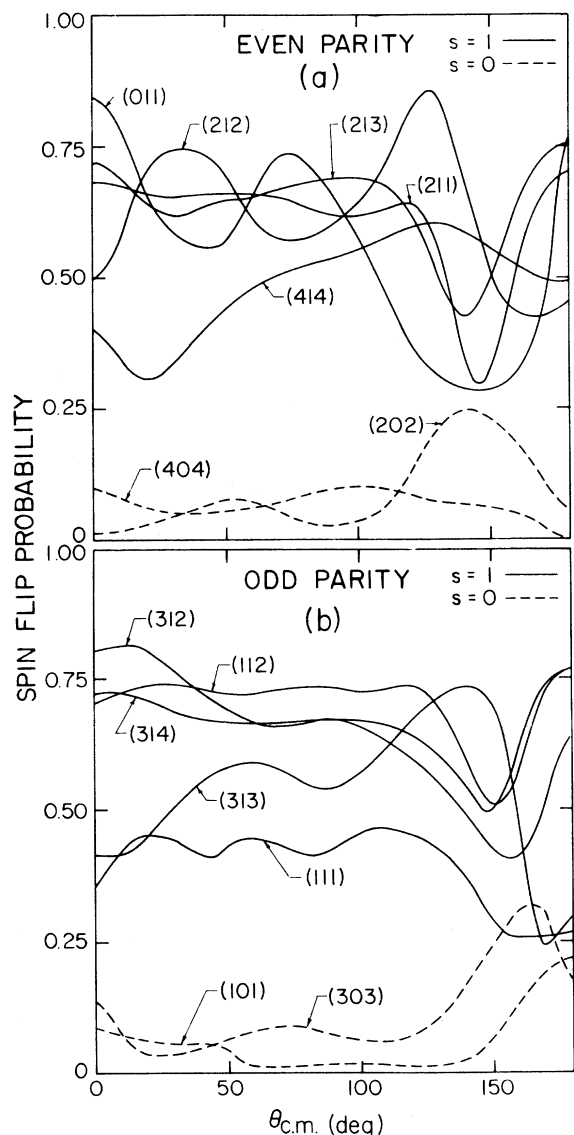


FIG. 1. Schematic DWBA calculations of the SF probability. The curves are labeled by their respective l , s , and j transfers.

cation for neglecting the $T_{3i}j_i$ term in the isovector operator is described in Ref. 7.) Neglecting exchange, the nuclear matrix elements for the central force direct contribution to inelastic scattering with $lsj = 011$ are

$$\text{isovector } I_1 = V_\sigma \sum_i \langle J_B T_B \| T_{3i} \tilde{\sigma}_i g_0(r, r_i) \| J_A T_A \rangle, \quad (1.6)$$

$$\text{isoscalar } I_0 = V_\sigma \sum_i \langle J_B T_B \| \tilde{\sigma}_i g_0(r, r_i) \| J_A T_A \rangle,$$

where V_σ and V_σ are the isovector and isoscalar component strengths of the spin-spin potential of

the N - N interaction (see Sec. III A) and g_0 is the zeroth order multipole expansion coefficient of the two-body interaction.

Isoscalar magnetic transitions are well known to be extremely weak since the coupling constant $\mu_+ = \mu_p + \mu_n - \frac{1}{2}$ is very small compared to $\mu_- = \mu_p - \mu_n + \frac{1}{2}$ ($\mu_+^2/\mu_-^2 = 0.0082$). To a lesser extent this rule also holds for higher multipolarity isoscalar magnetic transitions. In contrast, V_σ and V_σ are approximately the same size, resulting in comparable isoscalar and isovector excitation strength in inelastic scattering reactions. The other difference between Eqs. (1.5) and (1.6) is the presence of the radial function $g_0(r, r_1)$. In general, inelastic scattering operators will have a different radial dependence than the corresponding magnetic multipole cases. The very important angular dependence will, however, be very similar for the two types of operators characterized by the same l and j .

II. EXPERIMENTAL

A. General

In the past SF probabilities have been measured using the $(p, p'\gamma)$ technique.⁸ This technique works well for $J \leq 2$ states in even mass nuclei which have a strong gamma decay to a 0^+ state. The vast majority of $(p, p'\gamma)$ measurements have been performed on $0^+ - 2^+$ transitions where spin transfer is unobservably weak. Recently Howell *et al.*⁹ have demonstrated the potential of $(p, p'\gamma)$ technique for isovector transitions in a study of the $^{12}\text{C}(p, p')^{12}\text{C}$ (1^+ , $T = 1$, 15.11 MeV) reaction.

Most of the cases studied here could not have been performed with the $(p, p'\gamma)$ technique. Because of this, we have taken the more direct approach of measuring the polarization of the outgoing proton from a (p, p') reaction induced by an initially polarized beam. The crucial factor which made such experiments feasible was the development of a high resolution, high efficiency polarimeter.¹⁰ The polarimeter system, shown schematically in Fig. 2, employs an Enge split-pole spectrograph to achieve the desired momentum resolution as well as to eliminate unwanted reaction groups (particularly the elastically scattered protons). Details of the design and operation of the polarimeter are given in Ref. 10; we reiterate only the major points.

Following a nuclear interaction, the final proton polarization p_f , perpendicular to the reaction plane defined by \vec{k}_a and \vec{k}_b (normally denoted as the y direction, e.g., $\vec{y} = \vec{k}_a \times \vec{k}_b$), is a function of the initial proton polarization p_i and the analyzing power of the reaction, A_y ,

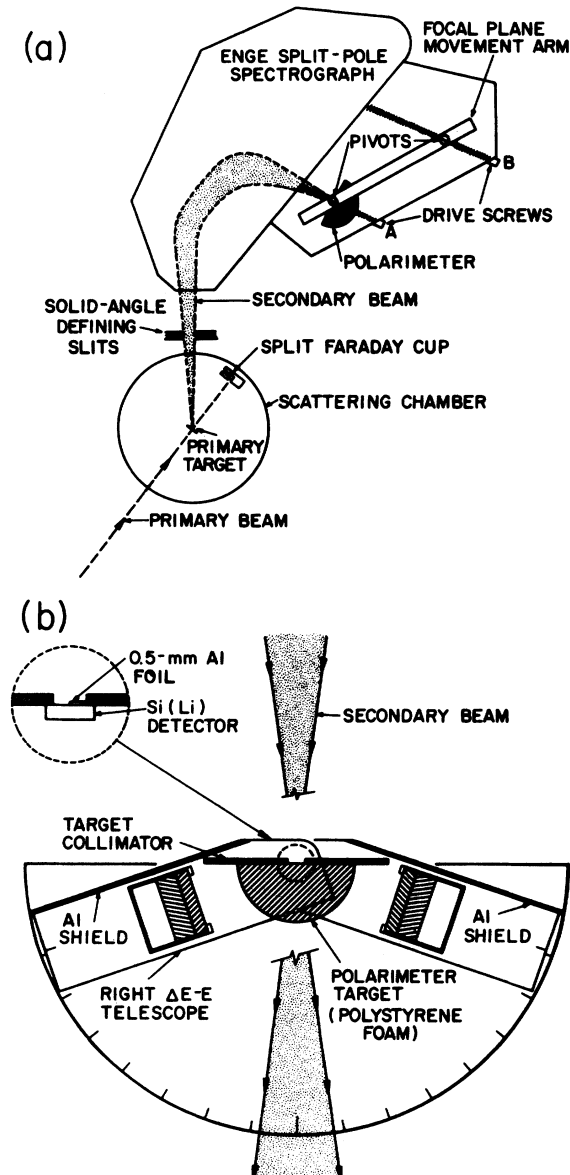


FIG. 2. Schematic layout of the spectrograph and focal-plane polarimeter.

$$p_f = \frac{P + p_i K_y^y}{1 + p_i A_y} \quad (2.1)$$

where P is the polarization function and K_y^y is the transverse polarization transfer coefficient.¹¹ Measurements of p_f with initial polarization both up (+) and down (-) lead to two equations from which P can be eliminated. One then has

$$K_y^y = \frac{(p_f^+ - p_f^-) - A_y(p_i^+ p_f^+ - p_i^- p_f^-)}{p_i^+ - p_i^-} \quad (2.2)$$

The SF probability is given by $S = \frac{1}{2} (1 - K_y^y)$.

B. Calibration and alignment

The final polarization is derived in the usual manner from the left-right asymmetry in the scattering from the polarimeter target. Specifically

$$p_f = \frac{1}{\bar{A}} \left(\frac{L - R}{L + R} \right), \quad (2.3)$$

where \bar{A} is the analyzing power of the polarimeter and L and R are the numbers of counts recorded in the left and right detector telescopes. The analyzing power has been measured both by direct scattering of the polarized proton beam (of known polarization) and by measuring the outgoing polarization in the $^{208}\text{Pb}(p, p)^{208}\text{Pb}$ reaction at small angles where Rutherford scattering dominates.

The crucial factor in the determination of p_f from Eq. (2.3) is the elimination of false asymmetries due to the misalignment of the polarimeter with respect to the centroid of the particle group impinging on the focal plane.¹⁰ The only part of the alignment procedure not described previously is the use of a solid state detector, shown in the dotted circle of Fig. 2(b). This replaces the two position-sensitive proportional counters used previously.¹⁰ The 5-mm-thick Si(Li) detector is mounted directly above the polarimeter and is collimated by the same collimator as the polarimeter target. Half of the detector aperture is covered with a 0.5-mm aluminum absorber. When a single state is centered on the target collimator, the spectrum from the detector consists of two peaks of equal area separated by 2 MeV. The polarimeter height is remotely controlled so that either the target or the centering device can be placed in position in the focal plane. During a run the centering of the peak on the polarimeter target is checked periodically.

C. Backgrounds and errors

The SF probabilities of several states must be corrected for background. These are the $^6\text{Li}(0^+ 3.56 \text{ MeV})$ and $^{12}\text{C}(1^+, 12.71 \text{ MeV})$ states which sit on a real continuum due to three body final state reactions, and the $^{14}\text{N}(1^+, 2.31 \text{ MeV})$ state which sits on a small tail from the elastic peak. In these cases corrections must be made to p_f in order to evaluate the real SF probability of the peak. We have made the plausible assumption that the spin-independent forces dominate in these processes and as a result $S \approx 0$. The final polarization associated with the background is then

$$p_f = \frac{A_y + p_i}{1 + p_i A_y}.$$

A measurement of A_y for the background above and below the peak of interest is made in order to correct the SF probability for the peak. Relaxing the assumption of $S=0$ for the background does not have a large effect on the final SF probability. For example, in the case of the $^{12}\text{C}(1^+, 12.71 \text{ MeV})$ state the SF probability would decrease by ~ 0.05 if $S_{\text{background}} = 0.25$.

The error bars reported here are determined by statistical errors only (including background subtraction when needed). We believe that, in general, systematic errors on S are less than 0.02. The data are shown in Figs. 3–14.

III. ANALYSIS AND DISCUSSION

A. Theoretical

The calculations presented in this section employ the microscopic DWBA and were performed with the code DWBA-70.¹² Effects due to exchange are included in all cases. Optical potentials taken from the literature are given in Table I.

In the microscopic DWBA the perturbing interaction which gives rise to inelastic scattering is the effective interaction between the incoming proton and each nucleon (i) of the nucleus. This can be written

$$\begin{aligned} V(\vec{r}, \vec{r}_i) = & V_0 + V_r \vec{\tau} \cdot \vec{\tau}_i + (V_\sigma + V_{\sigma r} \vec{\tau} \cdot \vec{\tau}_i) \vec{\sigma} \cdot \vec{\sigma}_i \\ & + (V_T + V_{T r} \vec{\tau} \cdot \vec{\tau}_i) S_{12} \\ & + \frac{1}{2} (V_{LS} + V_{LS r} \vec{\tau} \cdot \vec{\tau}_i) \vec{L} \cdot (\vec{\sigma} + \vec{\sigma}_i), \end{aligned} \quad (3.1)$$

where S_{12} is the usual tensor operator. As we have argued in Sec. I B substantial spin flip occurs only when the perturbing force explicitly depends on spin; we will therefore confine our

TABLE I. References for optical potentials. The energies for which the parameters were determined are given for both incoming and outgoing proton energies.

Nucleus	E proton (MeV)	Ref.	Comments
^6Li	32	13	$E_p = 29.9 \text{ MeV}$
^{11}B	31	14	$E_p = 30 \text{ MeV}$; Set A
^{12}C	42	15	$E_p = 40 \text{ MeV}$ incoming $E_p = 26.2 \text{ MeV}$ outgoing
^{14}N	34	16	$E_p = 31 \text{ MeV}$
^{15}N	40	17	$E_p = 39.7 \text{ MeV}$ incoming $E_p = 30.1 \text{ MeV}$ outgoing
^{16}O	40	17	$E_p = 39.7 \text{ MeV}$ incoming $E_p = 30.1 \text{ MeV}$ outgoing
^{40}Ca	35.5	18	$E_p = 35 \text{ MeV}$ incoming $E_p = 30 \text{ MeV}$ outgoing

attention to the last three terms of Eq. (3.1). Among these, the central spin-spin and tensor interactions are generally more important than the two-body spin-orbit interaction in producing spin flip.

It is possible to take a purely phenomenological view of the parameters of the N - N interaction. We have not done this, however, due to the complexity of the spin dependent N - N interaction and the relatively small amount of data available. A more fundamental approach is to use effective interactions derived from realistic free N - N interactions. In the calculations presented here, we have made extensive use of effective interactions derived¹⁹ from fits to the matrix elements of scattering operators obtained with a sum of Yukawa potentials to the analogous matrix elements of the Reid and Hamada-Johnston (HJ) potentials.

In this initial survey of spin flip in the (p, p') reaction we have concentrated on inelastic transitions where nuclear matrix elements should be reasonably well described by the shell model. The $1p$ shell nuclei are particularly well suited to this task. The Cohen and Kurath²⁰ (CK) wave functions give an excellent account of magnetic transition rates and, from the arguments outlined in Sec. I C, isovector (p, p') transitions with spin transfer should also be well described. For the isoscalar counterparts we have no reliable guide as to the accuracy of the shell-model transition densities. We shall see later that the largest discrepancies appear in this area.

Any hadronic reaction analysis suffers from the multiple uncertainties in the areas of reaction mechanisms, N - N interaction (including optical parameter vagaries), and nuclear wave functions. This is no less true with the SF probability, as observable. However, these uncertainties are decoupled to some extent by the hypothesis that spin flip is a reliable indicator of the action of spin-dependent forces. In the following discussion this hypothesis plays a prominent role. The following discussion includes some data which were presented previously in letter form.²⁻⁴

B. Unnatural parity transitions

1. Isoscalar transitions

Inelastic transitions of the type $0^+ \rightarrow J^\pi$ with $\pi = (-1)^{J+1}$ require spin transfer if a single-step reaction is assumed (neglecting the possibility of a dominant contribution from the two-body spin-orbit force). Following the argument of Sec. I B one therefore expects S to be large in these cases with the dominant excitation strength coming from the central spin-spin and tensor interactions.

The SF probability in the $^{12}\text{C}(p, p')^{12}\text{C}(1^+, 12.71 \text{ MeV})$ reaction at $E_p = 42 \text{ MeV}$ qualitatively confirms this expectation (Fig. 3). A major discrepancy appears, however, when the SF data and differential cross section data (from Ref. 21) are compared to an antisymmetrized DWBA calculation using the CK wave functions and the effective $N-N$ force derived from the Reid potential. The solid curves show reasonable agreement with $d\sigma/d\Omega$ (Fig. 4) but a substantial overprediction of S . The dominant excitation strength for the 1^+ state is predicted to arise from the tensor interaction primarily through the exchange amplitude. This is apparent when the tensor part of the interaction is set equal to zero (dashed curve). The calculated cross section is now far below experiment; however, the SF probability is well described. The sensitivity of S to optical parameter ambiguities is generally very small; for example, the solid curve of Fig. 3 changes to $S \approx 1$ for the entire forward angle range if the distorted waves are replaced by plane waves. Replacing the CK wave functions by single particle ($p_{3/2}^{-1}p_{1/2}$) wave functions likewise changes S very little. Thus the difference between the data and the full force (tensor dominated) calculations must be taken seriously. We have suggested previously³ that overprediction of S for the 1^+ ($T=0$) state of ^{12}C could be interpreted as evidence that the Reid-derived $N-N$ force contained a tensor term that was substantially too large. As we have seen, setting $V_T = V_{Tr} = 0$ gives good

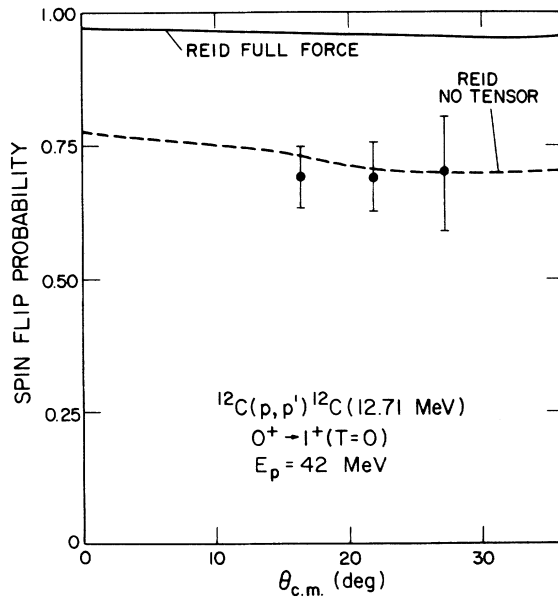


FIG. 3. Spin-flip probability for the 12.71 MeV state of ^{12}C . The curves are DWBA calculations described in the text.

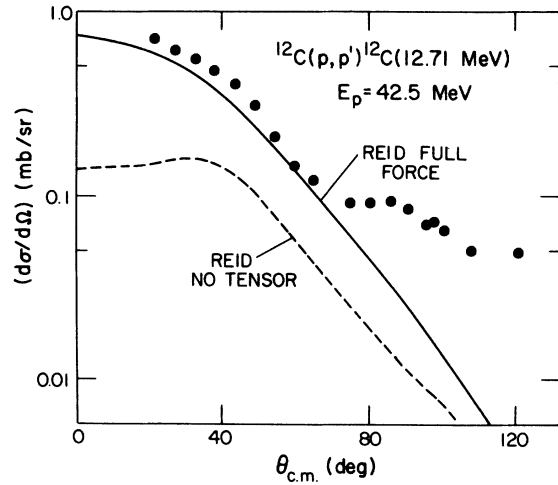


FIG. 4. Differential cross section data (from Ref. 21) for the 12.71 MeV state of ^{12}C . The curves are from DWBA calculations described in the text.

agreement with S , and the magnitude of $d\sigma/d\Omega$ may be regained by adjusting the strength of the central spin-spin potential. This is still a possibility but an alternative explanation seems more plausible from a study of the $2^-(8.88 \text{ MeV}, T=0)$ state of ^{16}O .⁴

Spin-flip and cross section data (the latter from Ref. 17) for the $^{16}\text{O}(p, p')^{16}\text{O}(2^-, 8.88 \text{ MeV})$ reaction at $E_p = 40 \text{ MeV}$ are shown in Figs. 5 and 6. The very small experimental values of S are in obvious disagreement with our simple connection

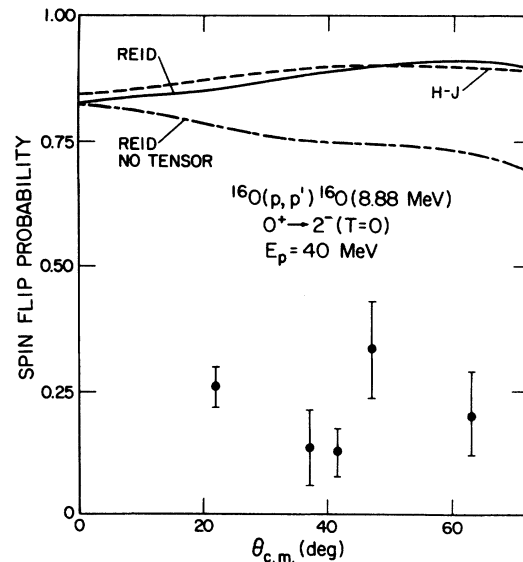


FIG. 5. Spin-flip probability for the 8.88 MeV state of ^{16}O . The curves are from DWBA calculations described in the text.

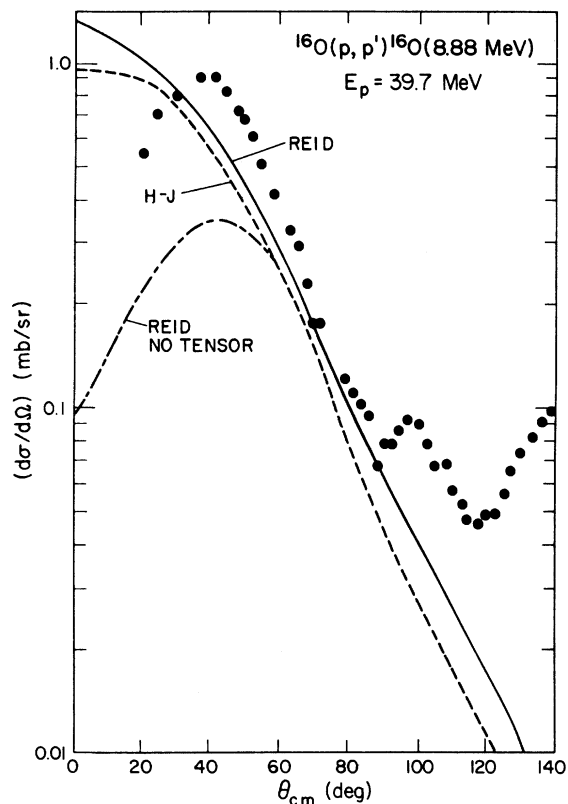


FIG. 6. Differential cross section data for the 8.88 MeV state of ^{16}O (from Ref. 17). The curves are from DWBA calculations described in the text.

between spin flip and the assumed spin transfer excitation of this state. The DWBA calculations for this reaction using the N - N forces from the Reid and HJ potentials and Gillet-Vinh Mau (GV) wave functions²² yield far too much spin flip and a rather poor description of the shape of the angular distribution. Again, by setting the tensor component of the N - N force equal to zero one sees the dominance of this term in the excitation strength of the 2^- state in ^{16}O . Contrary to the $^{12}\text{C}(1^+, T=0)$ case, however, the no-tensor calculation does not give substantially better agreement with the experimental SF probability.

As was suggested previously,⁴ we believe that the way out of this dilemma is to postulate the dominance of a more complex mechanism for the $^{16}\text{O}(p, p')^{16}\text{O}(2^-, 8.88 \text{ MeV})$ reaction at 40 MeV. The connection between spin-flip and spin transfer is taken seriously. Experimentally there is little spin flip, therefore there must be little contribution from direct single-step spin transfer. The more complex excitation may involve more than one mechanism. Possibilities include successive collective excitations proceeding through the $3^-(6.13 \text{ MeV})$ state or perhaps the virtual excita-

tion of giant resonances.²¹ In the absence of a specific model we made the assumption that the more complex mechanism does not depend on the spin of the proton and hence does not lead to spin flip. This is plausible on the general ground that the spin-independent parts N - N force are substantially larger than the spin dependent parts. With this assumption there is only a weak coherence between the spin transfer (s) and more complex paths (M) due to spin orbit distortion, and one may write

$$S_{\text{exp}} = \frac{S_s(d\sigma/d\Omega)_s + S_M(d\sigma/d\Omega)_M}{(d\sigma/d\Omega)_s + (d\sigma/d\Omega)_M} \approx S_s \frac{(d\sigma/d\Omega)_s}{(d\sigma/d\Omega)_{\text{exp}}},$$

since $S_M \approx 0$. One can then define the spin flip cross section $(d\sigma/d\Omega)_{\text{SF}}$

$$(d\sigma/d\Omega)_{\text{SF}} = S_{\text{exp}}(d\sigma/d\Omega)_{\text{exp}} \approx S_s(d\sigma/d\Omega)_s. \quad (3.2)$$

Without a model for the contribution of the complex mechanism to the total reaction strength, one cannot calculate S_{exp} ; however, $(d\sigma/d\Omega)_{\text{SF}}$ can be calculated.

The discrepancy between theoretical and experimental SF probabilities for the $^{12}\text{C}(1^+, T=0)$ state is less drastic but of the same type seen in ^{16}O . Thus we must reexamine both cases in light of the assumption made in Eq. (3.2). Spin-flip cross sections for the two reactions are shown together with DWBA calculations in Figs. 7 and 8. The modest overprediction for the $^{12}\text{C}(1^+, T=0)$ state results from a SF probability which is too large

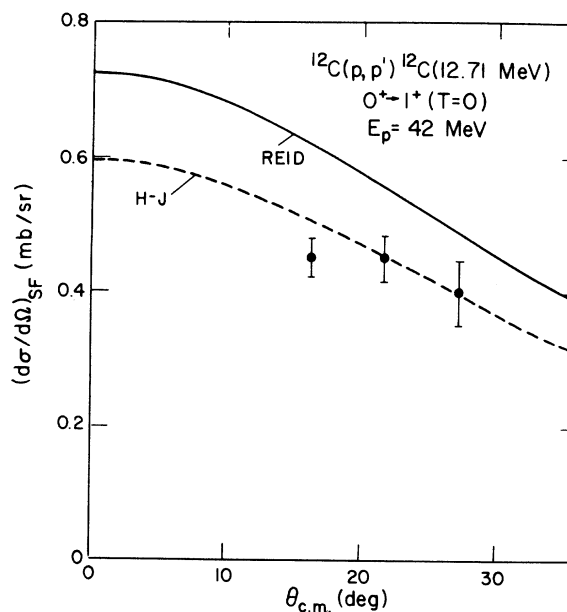


FIG. 7. Spin-flip cross section data for the 12.71 MeV state of ^{12}C . The curves are from DWBA calculations described in the text.

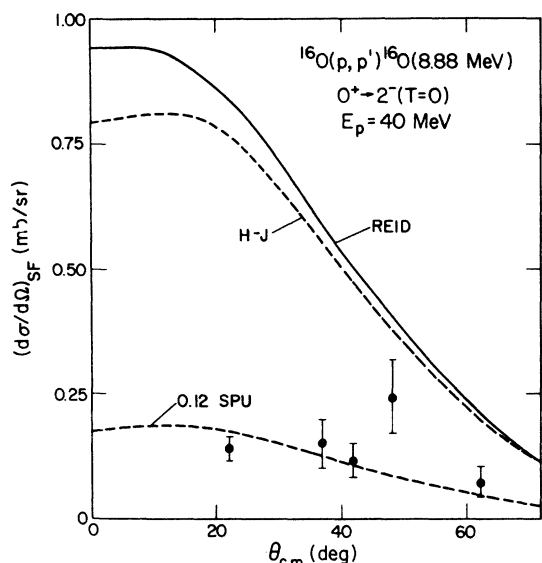


FIG. 8. Spin-flip cross section data for the 8.88 MeV state of ^{16}O . The upper curves are from DWBA calculations described in the text. The bottom curve has been normalized to the data.

and differential cross sections which are only slightly below the experimental values. Differences of the magnitude seen in Fig. 7 can be accommodated by numerous small adjustments of parameters. For example, calculation of $(d\sigma/d\Omega)_{\text{SF}}$ with a force derived from the HJ potential (dashed curve) fits the data very well.

In ^{16}O , however, there is substantial overprediction of $(d\sigma/d\Omega)_{\text{SF}}$. If one accepts the assumptions leading to Eq. (3.2), reaction mechanism difficulties have been taken out of the problem. The agreement seen in ^{12}C indicates that the HJ effective interaction is of the correct size. This leaves the GV wave functions used in the DWBA calculation as the source of the factor of 4–5 discrepancy between calculation and experiment.

The isoscalar spin-transfer matrix elements of the type which enter in the description of these states in ^{16}O and ^{12}C are not well known from other experiments. Electron scattering studies yield isovector magnetic transition rates which are clearly related to isovector transition strength in the (p, p') reaction (Sec. IC). Isoscalar magnetic transitions are severely inhibited due to the smallness of μ_+ (Sec. IC) and are consequently very poorly known. The large overprediction of $(d\sigma/d\Omega)_{\text{SF}}$ for the $^{16}\text{O}(2^-, T=0)$ state means that the GV wave functions yield an isoscalar “ $M2$ ” transition rate which is much too large. To be more quantitative we can express the theoretical and experimental enhancement factors in terms of DWBA calculations using a $(p_{1/2}^{-1}d_{5/2})_2$ - single

particle configuration. The GV wave functions give an isoscalar $M2$ strength of ~ 0.6 single particle units whereas normalization of the DWBA to the data (Fig. 8) yields ~ 0.12 single particle units.

The GV wave functions do not take into account the more complex configurations which are known to be present in the low-lying spectrum of ^{16}O . It has been suggested by G. E. Brown²³ that the small SF cross section may be a result of interfering contributions from the spherical and deformed components in the ground and 2^- states of ^{16}O . It would be extremely interesting to see if the Brown and Green²⁴ wave functions could account for the suppressed $M2$ strength as well as reproduce the spectroscopic factors for single nucleon transfer reactions leading to the 2^- state.

Unnatural parity $T=0$ states with “well-known” wave functions are rare. The $4^-(T=0, 5.61 \text{ MeV})$ state of ^{40}Ca , whose position is reasonably well predicted by the random phase approximation,²⁵ seemed a logical choice for further study of the problems seen in ^{16}O and ^{12}C . Unfortunately, on the experimental side, the 4^- state is nearly degenerate with a 2^+ state at 5.628 MeV. However, numerous SF studies of 2^+ states have revealed that at forward angles $S \leq 0.05$. One can write

$$S_{\text{exp}} = \frac{(d\sigma/d\Omega)_{2^+}(S_{2^+}) + (d\sigma/d\Omega)_{4^-}(S_{4^-})}{(d\sigma/d\Omega)_{\text{exp}}}$$

At $E_p = 35.5 \text{ MeV}$, $\theta_{\text{c.m.}} = 30^\circ$, Nolen and Gleitsman²⁶ have measured $d\sigma/d\Omega$ for the 2^+ and 4^- states with high resolution. With those values and the assumption $S_{2^+} = 0$ we can convert our measured S_{exp} at $E_p = 35 \text{ MeV}$, $\theta_{\text{c.m.}} = 30^\circ$, into S_{4^-} . (The additional error implied by $0 \leq S_{2^+} \leq 0.05$ has been incorporated into the error bars of S_{4^-} .) These data are compared to the calculations in Fig. 9. The error bar is large; however, one sees again that the SF probability is less than the theoretical values with or without the tensor term. The angular distribution is also not particularly well described by the full force calculations. Clearly, more precise SF probabilities are required before a definitive statement can be made about this case.

2. Isovector transitions

The SF probabilities for the $^6\text{Li}(p, p')^6\text{Li}(1^+ \rightarrow 0^+, T=1, 3.56 \text{ MeV})$ and $^{14}\text{N}(p, p')^{14}\text{N}(1^+ \rightarrow 0^+, T=1, 2.31 \text{ MeV})$ reactions are shown in Figs. 10 and 11. Although the errors are large, in both cases one sees a large S which is in agreement with the DWBA calculation. The two transitions which have the same initial and final J^π represent extremes in the excitation strength of the $l_{sj} = 011$ ($\tau = 1$) matrix element in the (p, p') reaction.

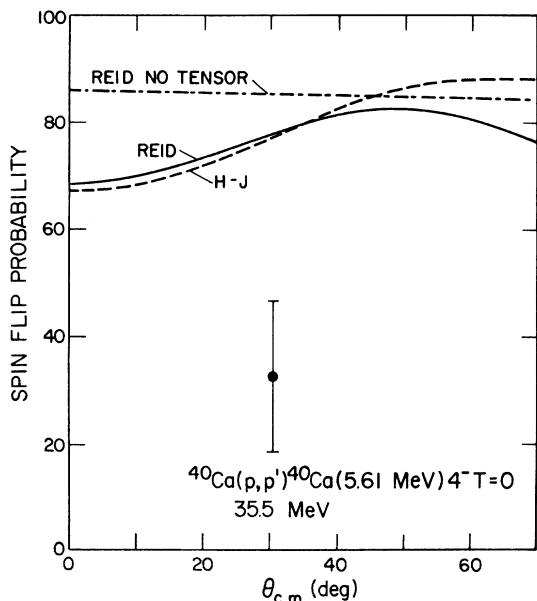


FIG. 9. Spin-flip probability for the 5.61 MeV state of ^{40}Ca . The curves are from DWBA calculations described in the text.

The large $B(M1)$ for the gamma-ray decay of the 0^+ to the ground state of ^6Li implies that the $lsj = 011$ matrix element in (p, p') will likewise be favored. The CK wave functions used in the present calculations describe the $M1$ strength adequately. The agreement between theory and experiment here is primarily an indication that this reaction is dominated by single-step spin transfer. Removal of the tensor force from the effective interaction changes the prediction of S only slightly. A substantial decrease in the errors would be difficult to achieve, because of the break-

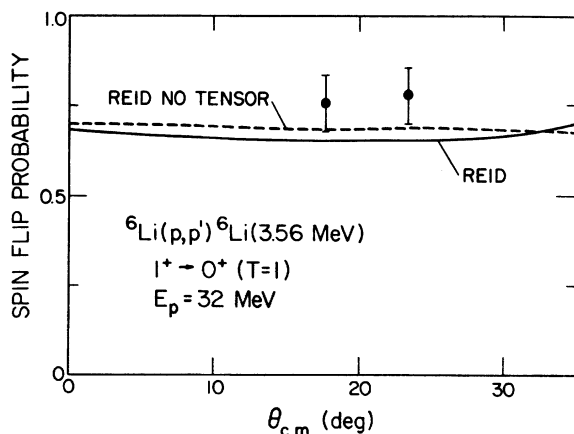


FIG. 10. Spin-flip probability for the 3.56 MeV state of ^6Li . The curves are from DWBA calculations described in the text.

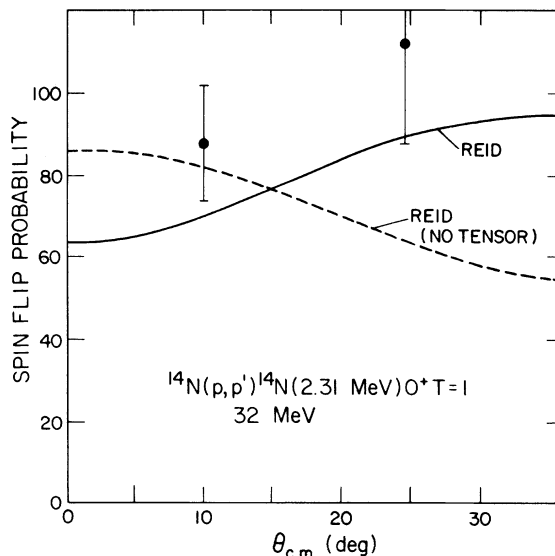


FIG. 11. Spin-flip probability for the 2.31 MeV state of ^{14}N . The curves are from DWBA calculations described in the text.

up continuum which underlies the 3.56 MeV state.

The $1^+ - 0^+$ transition in ^{14}N should have a vanishingly small $lsj = 011$ matrix element from the central spin-spin force. This follows from the close correspondence between the (p, p') excitation of the 0^+ state and the famous Gamow-Teller beta decay of ^{14}C .²⁷ This transition is thus favored ground for the observation of effects due to the tensor force. Crawley *et al.*²⁸ have shown that the very small differential cross section for this state is well described by the DWBA only if a tensor force is added to the $lsj = 211$ contribution of the central interaction. In view of the smallness of the cross section, contributions from more complex processes might also be of comparable magnitude. Following the reasoning presented in Sec. III B, a measurement of S should suffice to determine whether or not more complex processes are present. We note that the differential cross section was only $\approx 150 \mu\text{b/sr}$ at $\theta_L = 24^\circ$, where S was measured in the present experiment; this gives a good indication of the power of the present technique in the investigation of relatively weak spin-transfer transitions. The values of S shown in Fig. 11 indicate that spin transfer dominates the cross section for this transition. Although the errors in S do not permit a choice to be made between a dominance of the tensor force and the $lsj = 211$ central contribution only, this choice has already been made in favor of a sizable tensor force on the basis of the differential cross section.²⁸

C. Spin transfer in odd-mass nuclei

The nearly single-particle strength [$B(M1) = 0.8$ single particle units] for the $M1$ decay of the first excited state (2.14 MeV) of ^{11}B indicates a favored transition for $lsj = 011$ ($\tau = 1$) transfer in (p, p') . In odd mass nuclei, however, this is not a sufficient condition for a large SF probability, since transitions without spin transfer are always allowed as well. For the $\frac{3}{2}^- \rightarrow \frac{1}{2}^-$ transition in ^{11}B the allowed angular momenta are $lsj = 011, 211, 212,$ and 202 (with $\tau = 0$ or 1). The CK wave functions account well for the $M1$ decay of the 2.14 MeV state but do not contain a large enough configuration space to allow for the possible collectivity of an $lsj = 202$ "E2" type transition. It is therefore desirable to compare experiment and theory in terms of the SF cross section, where, because $S_{202} \approx 0$, the limited configuration space of the CK wave function should make little difference.

Figure 12 shows a comparison of the experimental SF cross section at $E_p = 32$ MeV with DWBA calculations using the CK wave function (cross section data from Ref. 29). The calculated $(d\sigma/d\Omega)_{\text{SF}}$ is very large due to the predicted dominance of the $lsj = 011$ "protonlike" nature of this transition. This is in obvious disagreement with the data which show evidence of very little spin transfer. The discrepancy between theory and experiment may be lessened by setting the tensor term to zero. However, at this point we have no justification for doing so. It seems more likely that the overprediction of $(d\sigma/d\Omega)_{\text{SF}}$ is due to inadequacy of the CK wave functions. There are several values which can contribute to this reaction for both $\tau = 1$ and $\tau = 0$ transfer; the $B(M1)$ tests only

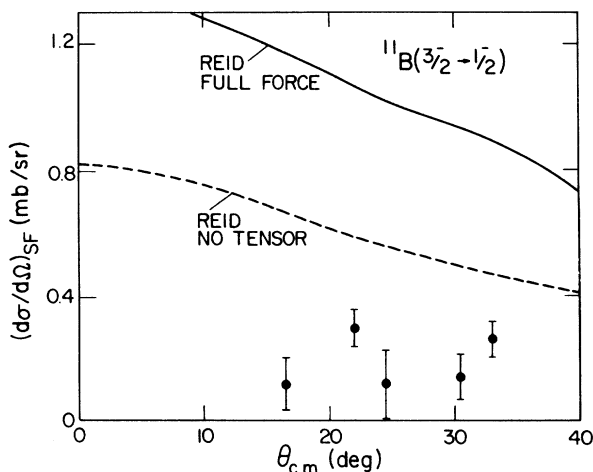


FIG. 12. Spin-flip cross sections for the 2.14 MeV state of ^{11}B at $E_p = 32$ MeV. The curves are from DWBA calculations described in the text.

one of these. It is possible that the small experimental SF cross section may result from a cancellation of the large 011 matrix element by one or more of the other terms. With this possibility it is of great interest to have calculations of $(d\sigma/d\Omega)_{\text{SF}}$ for this transition using wave functions derived from a larger shell-model basis.

The comments regarding ^{11}B can be equally well applied to the $^{15}\text{N}(\frac{1}{2}^- \rightarrow \frac{3}{2}^-)$, 6.32 MeV reaction at $E_p = 40$ MeV. Far too much SF cross section is predicted with either the Reid or HJ interactions (Fig. 13) in conjunction with an assumed $p_{1/2} \rightarrow p_{3/2}$ proton hole transition. Electron scattering measurements of the $M1$ rate for this transition yield somewhat less than the single particle value (0.64 Weisskopf units). Reduction of the calculated curves by this value still leaves about a factor of 2 too much SF cross section.

D. Spin flip in collective transitions

Numerous $(p, p'\gamma)$ experiments have shown that for collective transitions the forward angle ($\theta_{\text{c.m.}} \leq 90^\circ$) SF probability is close to zero; hence we have not devoted a great deal of time to additional verifications of this fact. Figure 14 shows SF measurements on two collective transitions, $^6\text{Li}(p, p')^6\text{Li}$ ($1^+ \rightarrow 3^+$, 2.18 MeV) and $^9\text{Be}(p, p')^9\text{Be}$ ($\frac{3}{2}^- \rightarrow \frac{5}{2}^-$, 2.43 MeV), which cannot be studied by $(p, p'\gamma)$. Both reactions are dominated by $lsj = 202$ collective strength and have SF probabilities consistent with effects due to spin-orbit distortion and ground-state quadrupole deformation alone.³⁰

IV. SUMMARY

This work represents the first extensive application of polarization transfer techniques to the study of the (p, p') reaction. The experimental observable, the SF probability, has been shown

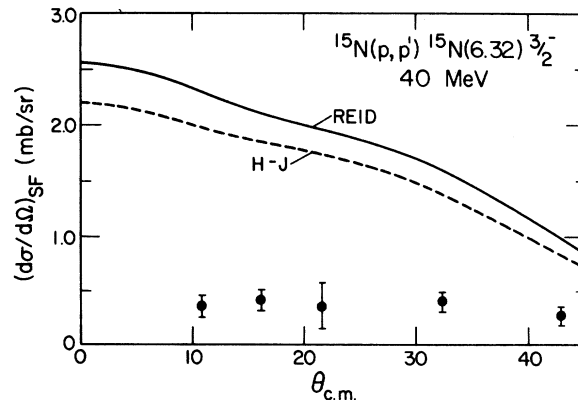


FIG. 13. Spin-flip cross sections for the 6.32 MeV state of ^{15}N . The curves are from DWBA calculations described in the text.

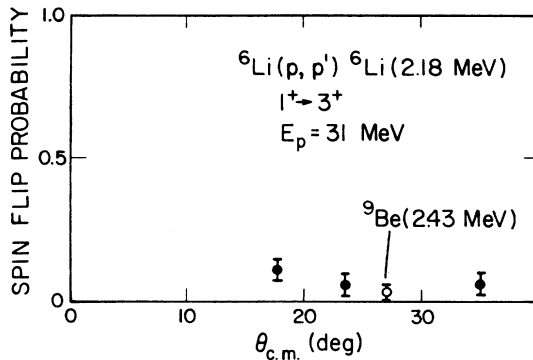


FIG. 14. Spin-flip probabilities for states in ${}^6\text{Li}$ and ${}^9\text{Be}$. The solid points are for ${}^6\text{Li}$ and the open point is for ${}^9\text{Be}$.

to be very closely related to spin transfer in inelastic scattering. When spin transfer is dominant a large SF probability should be observed; conversely in reactions where spin transfer is small or absent, the SF probability should be close to zero.

Antisymmetrized DWBA calculations reproduce the SF probability data only in the case of the isovector $1^+ \rightarrow 0^+$ transitions in ${}^6\text{Li}$ and ${}^{14}\text{N}$ (the

only isovector cases studied). Large discrepancies between theory and experiment are seen in the isoscalar transitions ${}^{12}\text{C}(0^+ \rightarrow 1^+, 12.71 \text{ MeV})$, ${}^{16}\text{O}(0^+ \rightarrow 2^-, 8.89 \text{ MeV})$, and ${}^{40}\text{Ca}(0^+ \rightarrow 4^-, 5.61 \text{ MeV})$. This has been interpreted as evidence of more complex, spin-independent, multistep reactions competing with direct spin transfer. In these cases and in the transitions in odd mass nuclei, the SF cross section becomes a more meaningful test of theory. Comparison of experimental SF cross sections to calculations for ${}^{11}\text{B}$, ${}^{15}\text{N}$, and ${}^{16}\text{O}$ reveal additional and, as yet, unexplained discrepancies.

This work is only beginning of the application of polarization transfer techniques to inelastic proton scattering. The spin dependence of the N - N interaction at low ($E < 100 \text{ MeV}$) and intermediate ($E > 100 \text{ MeV}$) energies and the investigation of spin transfer matrix elements in nuclear structure are topics of continuing interest. We believe that the spin-flip probability will become an observable of major importance in the investigation of these areas of nuclear physics.

This work was supported in part by the National Science Foundation and the Robert Welch Foundation.

*Present address: Los Alamos Scientific Laboratory, Los Alamos, N.M. 87545.

¹H. Sherif and J. S. Blair, Phys. Lett. **26B**, 489 (1968).

²J. M. Moss, W. D. Cornelius, and D. R. Brown, Phys. Lett. **69B**, 154 (1977).

³J. M. Moss, W. D. Cornelius, and D. R. Brown, Phys. Lett. **71B**, 87 (1977).

⁴J. M. Moss, W. D. Cornelius, and D. R. Brown, Phys. Rev. Lett. **41**, 930 (1978).

⁵G. R. Satchler, Nucl. Phys. **55**, 1 (1964).

⁶M. Kawai, T. Terasawa, and K. Izumo, Nucl. Phys. **59**, 289 (1964).

⁷E. K. Warburton and J. Weneser, in *Isospin in Nuclear Physics*, edited by D. H. Wilkinson (North-Holland, Amsterdam, 1969), p. 173.

⁸F. H. Schmidt, R. E. Brown, J. B. Gerhart, and W. A. Kolasinski, Nucl. Phys. **52**, 353 (1964).

⁹R. H. Howell, F. S. Dietrich, D. W. Heikkinen, and F. Petrovich, Phys. Rev. C **21**, 1153 (1980).

¹⁰J. M. Moss, D. R. Brown, and W. D. Cornelius, Nucl. Instrum. Methods **135**, 139 (1976).

¹¹G. G. Ohlsen, Rep. Prog. Phys. **35**, 717 (1972).

¹²R. Schaeffer and J. Raynal (unpublished).

¹³K. H. Bray, J. Jain, K. S. Jayaraman, G. Lobianco, G. A. Moss, W. T. H. van Oers, D. O. Wells, and F. Petrovich, Nucl. Phys. **A189**, 35 (1972).

¹⁴J. F. Cavignac, S. Jang, and D. H. Worledge, Nucl. Phys. **A243**, 349 (1975).

¹⁵J. J. Kolata and A. Galonsky, Phys. Rev. **182**, 1073 (1969).

¹⁶C. C. Kim, S. M. Bunch, D. W. Devins, and H. H. Forster, Nucl. Phys. **58**, 32 (1964).

¹⁷S. M. Austin, P. J. Locard, S. N. Bunker, J. M. Cameron, J. R. Richardson, J. W. Verba, and W. T. H. van Oers, Phys. Rev. C **3**, 1514 (1971).

¹⁸H. V. Geramb and P. E. Hodgson, Nucl. Phys. **A246**, 172 (1975).

¹⁹G. Bertsch, J. Borysowicz, H. McManus, and W. G. Love, Nucl. Phys. **A284**, 399 (1977).

²⁰S. Cohen and D. Kurath, Nucl. Phys. **73**, 1 (1965).

²¹H. V. Geramb, K. Amos, R. Sprickman, K. T. Knöpfle, M. Rogge, D. Ingham, and C. Mayer-Boricke, Phys. Rev. C **12**, 1697 (1975).

²²V. Gillet and N. Vinh Mau, Nucl. Phys. **54**, 321 (1964).

²³G. E. Brown (private communication).

²⁴G. E. Brown and A. M. Green, Phys. Lett. **15**, 168 (1965).

²⁵W. J. Grace and A. M. Green, Nucl. Phys. **A113**, 641 (1968).

²⁶J. A. Nolen and R. J. Gleitsman, Phys. Rev. C **11**, 1159 (1975).

²⁷W. M. Visscher and R. A. Ferrell, Phys. Rev. **107**, 781 (1957).

²⁸G. M. Crawley, S. M. Austin, W. Benenson, V. A. Madson, F. A. Schmittroth, and M. J. Stomp, Phys. Lett. **32B**, 92 (1970).

²⁹J. Lowe, Nucl. Phys. **A162**, 438 (1971).

³⁰J. S. Blair, M. P. Baker, and H. S. Sherif, Phys. Lett. **60**, 25 (1975).

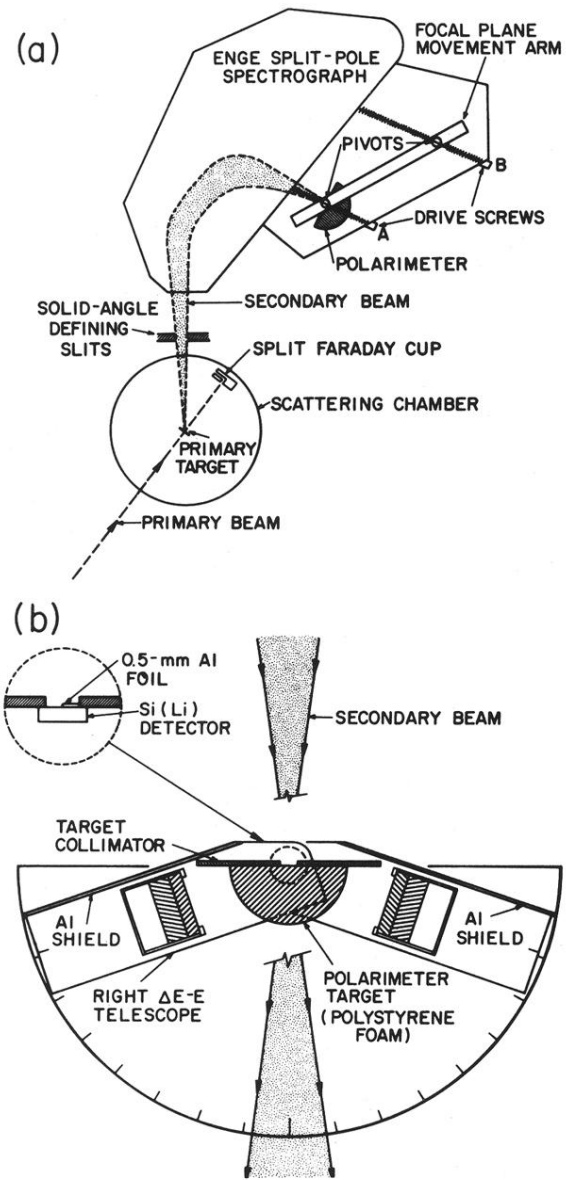


FIG. 2. Schematic layout of the spectrograph and focal-plane polarimeter.